



# Improving the quantification of peak concentrations for air quality sensors via data weighting

Caroline Frischmon<sup>1,★</sup>, Jonathan Silberstein<sup>1,★</sup>, Annamarie Guth<sup>1</sup>, Erick Mattson<sup>2</sup>, Jack Porter<sup>3</sup>, and Michael Hannigan<sup>1</sup>

<sup>1</sup>Department of Mechanical Engineering, University of Colorado Boulder, 1111 Engineering Drive, Boulder, CO 80309, USA

<sup>2</sup>Colorado Department of Public Health and Environment, 4300 Cherry Creek Drive South, Glendale, CO 80246, USA

<sup>3</sup>South Coast Air Quality Monitoring District, 21865 Copley Drive Diamond Bar, CA 91765, USA

★These authors contributed equally to this work.

**Correspondence:** Caroline Frischmon (caroline.frischmon@colorado.edu)

Received: 23 December 2024 – Discussion started: 22 January 2025

Revised: 25 March 2025 – Accepted: 27 April 2025 – Published: 15 July 2025

**Abstract.** Traditional calibration models for low-cost air quality sensors have demonstrated a tendency to underpredict peak concentrations. We assessed the utility of adding data weights to low-cost sensor colocation data to improve the quantification of peak concentrations when the majority of colocation data is at a baseline concentration and varies due to intermittent, transient events. Specifically, we explore the effects of data weighting on three different pollutant colocation datasets: total volatile organic compounds (VOCs), carbon monoxide (CO), and methane (CH<sub>4</sub>). Leveraging two different weighting functions, a sigmoidal and a piecewise weighting regime, we explored the impacts of the base model choice (multilinear regression, MLR, vs. random forest, RF, models), the sensitivity of weighting functions, and the ability of data weighting to improve high-concentration pollution measurements. When compared to unweighted colocation data, we demonstrate significant reductions in both error (root mean square error, RMSE) and bias (mean bias error, MBE) for pollutant peaks across all three datasets when data weighting is employed. For the top percentile of data, we observe an average of 23 % reduction in RMSE and a 35 % reduction in MBE when optimal weights are employed. More significant reductions occurred in the 95th–99th percentile of data, where MBE was reduced by an average of 70 %. RMSE in the 95th–99th percentile was reduced by an average of 26 %. However, data weighting can also generate larger errors at baseline pollutant concentrations. Data weighting regimes were sensitive to input parameters, and input weighting functions may be tuned to better predict peak concen-

tration data without significant reductions in the fidelity of baseline pollutant predictions.

## 1 Introduction

Over the past several decades, advances in both sensor technology and quantification methods have allowed for low-cost sensor (LCS) networks to accurately quantify spatiotemporal changes in pollutant concentrations (Okorn and Hannigan, 2021a; Thorson et al., 2019; Karagulian et al., 2019). These sensors are often simple to deploy, making them well suited to a wide variety of monitoring applications. For a fraction of the cost of a single regulatory monitor, several LCSs may be deployed across the monitoring area of interest, allowing for a more granular picture of local air quality (Morawska et al., 2018; Casey and Hannigan, 2018; Collier-Oxandale et al., 2018).

In many areas, sources of air pollution are often numerous, transient, and/or highly localized, requiring a wide suite of LCSs to predict concentrations of relevant pollutants. Elevated concentrations of air pollutants such as volatile organic compounds (VOCs), methane (CH<sub>4</sub>), and carbon monoxide (CO) can result in a series of adverse health and environmental outcomes (Zhou et al., 2023; Zhang et al., 2017). The health impacts of CO and VOC exposure include cardiopulmonary and respiratory illnesses and other forms of increased morbidity (Xing et al., 2016; Raub, 1999; Halios et al., 2022;

Liu et al., 2022). CH<sub>4</sub> emissions result in significant contributions to the anthropogenic greenhouse gas budget, accelerating the impacts of climate change. Accurate assessment of the concentrations of these pollutants is essential in characterizing exposure, mitigating fugitive greenhouse gas emissions, and identifying areas of enhanced pollution.

LCSs require extensive calibration to accurately predict air pollutant concentrations. As LCS signal may be affected by drift over time, changes in temperature and humidity, and cross-sensitivity to other pollutants, the raw sensor signal is often calibrated to ensure reliable measurements (Wei et al., 2018; Tancev, 2021; Rai et al., 2017; Sayahi et al., 2019; Mei et al., 2020; Jayaratne et al., 2018; Malings et al., 2020). Typically, LCSs are calibrated via a procedure known as colocation – a process where sensors are placed adjacent to a reference grade monitor for an extended period. A regression model is developed to fit the raw sensor signal to the measured concentrations of the reference monitor over the colocation period (Okorn and Hannigan, 2021b; Levy Zamora et al., 2023). For large datasets spanning data from multiple sensors under varying air pollutant concentrations, researchers have developed correction algorithms to improve sensor signal during extreme events, though these correction factors require significant data and extensive testing (Barkjohn et al., 2021). Other methods for calibrating LCSs, such as measuring sensor response to a target pollutant in a laboratory setting, may be poorly suited for field applications. The range of environmental parameters and chemical composition of the local environment may vary dramatically between a lab setting and field deployment of a LCS, resulting in large errors in predicted pollutant concentrations when lab calibrations are applied (Liang, 2021; Gonzalez et al., 2019).

Even in areas experiencing elevated air pollution, the majority of ambient LCS signals is often near-baseline, measuring relatively low pollutant concentrations (Collier-Oxandale et al., 2018; Casey et al., 2019; Sayahi et al., 2019; Bigi et al., 2018). LCSs capture significantly elevated concentrations of air pollutants during short-term “spikes” when sampling a plume from a pollution source (Mead et al., 2013). In the majority of LCS calibration models, both baseline data points and high-concentration pollution spikes are given equal weights. However, as most ambient LCS data are near baseline, calibration model solutions may generate coefficients that fit the baseline well but result in large errors when predicting higher-concentration pollution spikes (Okorn and Hannigan, 2021a). Furthermore, this unweighted calibration procedure may result in residuals that display significant biases at high concentrations, resulting in concentrations of predicted pollutants that are systematically lower or higher during concentration peaks than is physically accurate (Collier-Oxandale et al., 2018; Silberstein et al., 2024; Magi et al., 2020; Zimmerman et al., 2018).

For many LCS applications, including environmental justice analyses, industrial leak or event detection, wildfire

plume quantification, and urban air pollution assessment, accurately quantifying pollutant spikes during elevated emission events is often the primary concern. To improve the fitting of high-concentration peaks during LCS calibration, additional model weights may be required. Data weighting is commonly employed in other environmental applications, including geospatial air pollution analysis (Rose et al., 2009; De Mesnard, 2013; Liu et al., 2019) and hotspot identification (Bi et al., 2020). Other forms of data modification, such as data downsampling and upsampling, have been employed for LCS calibration (Tang et al., 2024). However, downsampling techniques often require considerable data, and the size of the final dataset employed in calibration is significantly downsampled (Furuta et al., 2022; Silberstein et al., 2024). Conversely, upsampling can often result in overfitting as the technique adds duplicates for underrepresented data (Susan and Kumar, 2021).

In characterizing the performance of both calibration models and sensors during colocation, researchers employ statistical metrics such as the error and bias to assess the efficacy of LCS equipment (Casey et al., 2019; Sadighi et al., 2018). However, these metrics are calculated using the entire colocation dataset, which may neglect for significant variability in error and bias across differing pollutant concentrations. As near-baseline pollutant concentrations comprise the majority of colocation data, large errors and biases during pollutant spikes typically have little effect on overall model performance. Consequently, researchers may overlook poor model fits at higher pollutant concentrations. Fields such as data science routinely employ weights to optimize for certain portions of a sample dataset. Our objective in this paper is to develop a methodology for the implementation of data weights in LCS applications and to characterize the strengths and limitations of various weighting techniques. To our knowledge, this study represents the first application of LCS model weighting during colocation to improve sensor prediction of peak pollutant concentrations.

## 2 Methods

To study the efficacy of data weighting in sensor calibration models, we applied weights to three distinct datasets collected during low-cost sensor (LCS) colocations with reference instrumentation and compared the weighted model outcomes to the unweighted counterparts. For each colocation dataset, we tested two weighting schemes with two calibration model types to explore how various factors impact the weighted model predictions. The LCS data, reference data, weighting schemes, and calibration models are detailed below.

## 2.1 Instrumentation

LCS measurements were collected via HAQPods, a low-cost air quality monitor developed by the Hannigan Lab that integrates several commercially available sensors (Hannigan Lab, Boulder, Colorado). Briefly, CO measurements were collected by an Alphasense CO-B4 sensor (Alphasense, Braintree, United Kingdom), TVOC measurements were collected via a Figaro 2600, a Figaro 2611, and two Figaro 2602 sensors (Figaro, Rolling Meadows, Illinois). Methane measurements were collected using the same sensors as the TVOC measurements, in addition to an MQ4 (Hanwei Electronics, Zhengzhou, China). The approximate cost, sensing range, and target pollutant of each sensor are given in Table S1 in the Supplement.

## 2.2 Colocation description

A single HAQPod was deployed for colocation at each of the three field sites across California and Colorado (Fig. 1). CO sensors were calibrated via an approximately 10-week field colocation with a reference 48i-TLE CO (Thermo Scientific) monitor. The CO colocation field site was located directly adjacent to Interstate 25, a major highway (Fig. 1). Reference monitors were maintained by the Colorado Department of Public Health and Environment (CDPHE). CH<sub>4</sub> sensors were calibrated via a 5-month colocation with reference Picarro CH<sub>4</sub>–H<sub>2</sub>S Analyzer at a South Coast Air Quality Management District (South Coast AQMD) site in Huntington Park, CA (Fig. 1). TVOC sensors were calibrated with a reference FTIR continuous optical multi-pollutant analyzer (FluxSense Inc., San Diego, CA) for 5 months at a site in Long Beach, CA, maintained by South Coast AQMD.

The LCS signal data were *z*-scored and time-averaged using median values in 5 min increments. We also applied this time-averaging to the reference data. Maximum reference CO concentrations over the colocation period were 1.84 ppm, and minimum reference concentrations were 0.04 ppm (Fig. 2). Maximum and minimum reference CH<sub>4</sub> concentrations were 8.75 and 1.96 ppm. For TVOC, reference concentrations ranged from below the detection limit of 15 to 2978 ppb.

## 2.3 Calibration models

### 2.3.1 Multilinear regression (MLR)

MLR employs several independent variables to predict a dependent variable. In the context of LCS calibration, the independent variables correspond to individual *z*-scored sensor signals, and the dependent variable corresponds to measured concentrations of an air pollutant by the reference instrument. Multilinear regression can be expressed as

$$y_i = \beta_0 + \sum_{j=1}^p \beta_j x_{ij} + \epsilon_i, \quad (1)$$

where  $\beta$ s represent the model regression coefficients,  $y$  is the response for the  $i$ th observation,  $x_{ij}$  is the  $j$ th predictor variable for the  $i$ th observation, and  $\epsilon_i$  represents the error term for the  $i$ th observation. For a weighted multilinear regression, the error term is defined as the weighted sum of squared residuals (SSRs):

$$\text{Weighted SSR} = \sum_{j=1}^p W_i (y_i - \hat{y}_i)^2, \quad (2)$$

where  $y_i$  is again the response for the  $i$ th observation,  $\hat{y}_i$  is the predicted response for the  $i$ th observation, and  $W_i$  is the weight applied to the  $i$ th observation in a weighted model. The model coefficients are tuned by minimizing the SSR.

MLR models are often employed in LCS applications when sensor behavior is linear over a specific range of air pollutants and environmental parameters. MLR models are well suited for small training datasets as they tend to overfit training data less than machine learning models.

### 2.3.2 Random forest (RF)

RF models represent a more complex alternative to MLR models. These models have previously been employed in higher complexity LCS datasets that contain extensive colocation data (Zimmerman et al., 2018). These models are composed of several decision trees, and the final RF model prediction is influenced by the predictions of each of the individual trees. As an ensemble model, RF predictions are less likely to be overfit than a single prediction from any individual decision tree. Machine learning models such as RFs require tuning of hyperparameters, including the number of decision trees, number of estimators, and minimum leaf size. Hyperparameters were determined for each pollutant colocation dataset via the minimization of the root mean squared error. Additional information regarding RF models can be found in other manuscripts (Zimmerman et al., 2018; Karagulian et al., 2019). The error term (weighted RMSE) for a weighted random forest model is defined in Eq. (3).

$$\text{Weighted RMSE} = \sqrt{\frac{\sum_{i=1}^n W_i (y_i - \hat{y}_i)^2}{\sum_{i=1}^n W_i}} \quad (3)$$

## 2.4 Data weighting functions

To assess the strengths and limitations of different methods for weighting colocation data, we tested two variants of weighting functions on our data. Assessed weighting functions are displayed in Fig. 3. These functions are discussed in detail below.

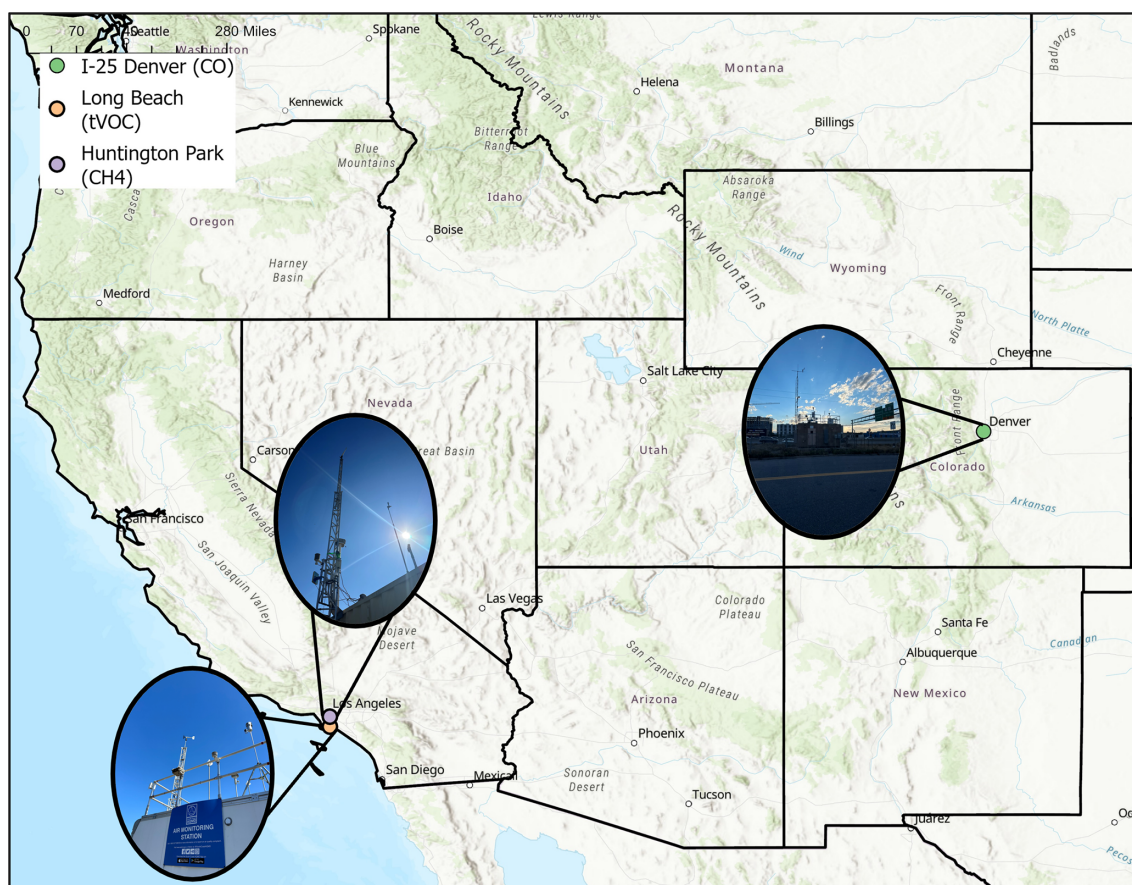


**Figure 1.** Colocation site map for the three study sites shown as colored circles (ArcGIS, ESRI). Images of each field site are displayed alongside each site.

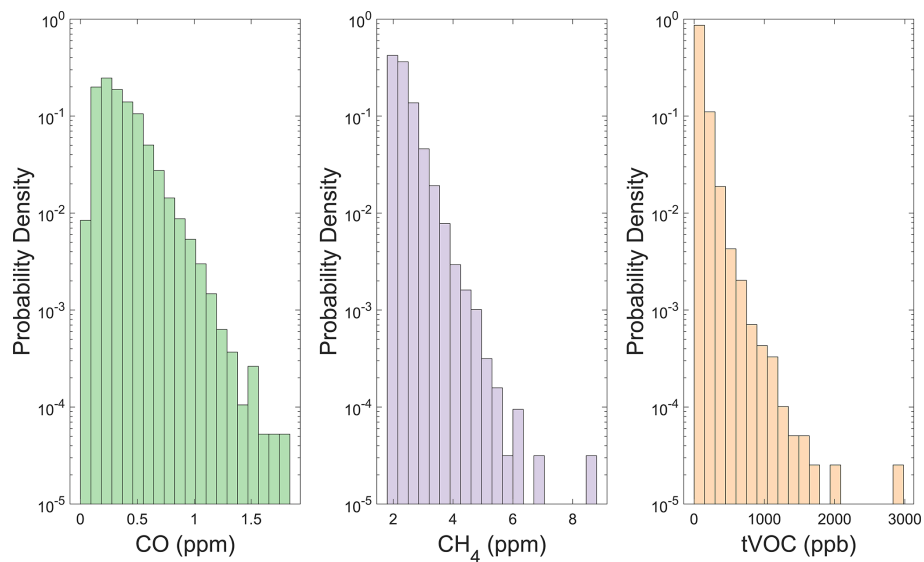


**Figure 2.** Reference measurement pollutant concentration distributions for CO (green), CH<sub>4</sub> (purple), and TVOC (orange) measurements. Probability density of each concentration bin is displayed on a log scale.

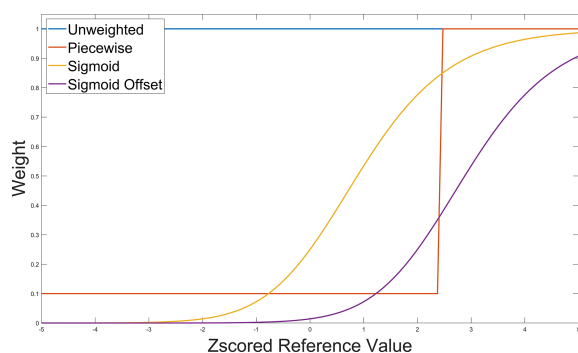


**Figure 3.** Weighting functions employed in this study as a function of  $z$ -scored reference measurement. Example unweighted (blue), piecewise (orange), sigmoidal (yellow), and sigmoidal with an offset (purple) weighting curves are shown.

### 2.4.1 Sigmoidal weights

A sigmoidal squared offset weighting distribution given in Eq. (4) was applied. Reference data were then assigned weights as follows:

$$W(z) = \frac{1}{(1 + e^{-z+X})^2}, \quad (4)$$

where  $z$  represents the  $z$ -scored value of a reference monitor concentration and  $X$  is the user input offset for the function. The offset,  $X$ , shifts the weighting distribution to higher- or lower- $z$ -scored values depending on user preference. In Sect. 2.6, we analyzed the model sensitivity to offsets ranging from 0–3.

### 2.4.2 Piecewise weights

The simplest weighting method explored in this study leverages piecewise weights as shown in Eq. (5). Reference data ( $y_i$ ) above a certain percentile,  $P$ , were given a weight of 1, while data below the percentile were given a weight of 0.1. In Sect. 2.6, we tested the sensitivity of our piecewise weighting scheme to percentile set points ranging from the 75th–99.9th percentile.

$$W(z) = \begin{cases} 0.1, & z \leq P \\ 1, & z > P \end{cases} \quad (5)$$

## 2.5 Data analysis frameworks

The LCS-predicted concentrations were segregated into percentile ranges, based on the corresponding reference concentrations, to better understand the impacts of data weighting on low-, average-, and high-concentration (peak) data. Data were grouped in the 0th–5th, 5th–25th, 25th–75th, 75–95th, 95th–99th, and 99th–100th percentiles. Model performance was assessed as a function of mean bias error and root mean

squared error. As only a subset of fitting statistics are discussed in the subsequent sections, we provide the full fitting statistics for MLR and RF models in Tables S2–S4. For CO and CH<sub>4</sub>, the first and last 10 % of data were used excluded from model training to test the models' ability to predict concentrations under unseen conditions. These data are hence referred to as testing data. For the TVOC dataset, the last 20 % was used as testing data to achieve more peaks within the testing dataset.

## 2.6 Sensitivity analyses and colocation application

To understand how our regression solutions change as the parameters of the weighting functions are altered, we conducted a sensitivity analysis. We varied the linear offset,  $X$ , or percentile set point,  $P$ , of the sigmoidal and piecewise weighting function, respectively, to understand how predicted air pollutant concentrations changed. To conduct this sensitivity analysis, we varied the offset in intervals of 0.5 between values of 0 and 3.0 for sigmoidal weights and varied the percentile set point to the 75th, 80th, 85th, 90th, 95th, 99th, 99.5th, and 99.9th percentiles for piecewise weights.

Assessing the uncertainty associated with predicted air pollutant concentrations is often complex as errors and biases may be influenced by a combination of sensor performance, model choice, and distribution of pollutant concentrations. For each of the previously discussed colocation datasets, we plotted the RMSE and MBE as a function of the reference data concentration percentile to understand the sensitivity of errors and biases to changes in weighting offsets or percentile set points. For visual clarity, Figs. 4, 6, and 8 show the RMSE and MBE for only a subset of the tested offsets and percentile set points using the ideal model type (RF or MLR) for each pollutant. Plots with all tested models displayed are provided in the Supplement (Figs. S1–S6). In subsequent analyses, we further investigated the weighting functions that improved high-concentration fitting.

Using the optimal weighting functions, we then investigated how our predicted concentrations changed over the field colocation when data weighting was implemented.

## 3 Results and discussion

### 3.1 CO sensitivity analysis and colocation application

According to our sensitivity analysis, MLR models were better suited to the CO dataset when weights were applied (Figs. 4 and S1–S2). As shown in Fig. 4 below, piecewise weighting functions outperformed unweighted MLR models at elevated concentrations of CO, with minimal degradation in performance at lower concentrations (Fig. 4, Tables S2–S4). Sigmoidal weighting functions displayed increased sensitivity to input parameters at lower concentrations of CO and displayed lower RMSE and greater biases than piecewise weights. These results indicate that assessing multiple



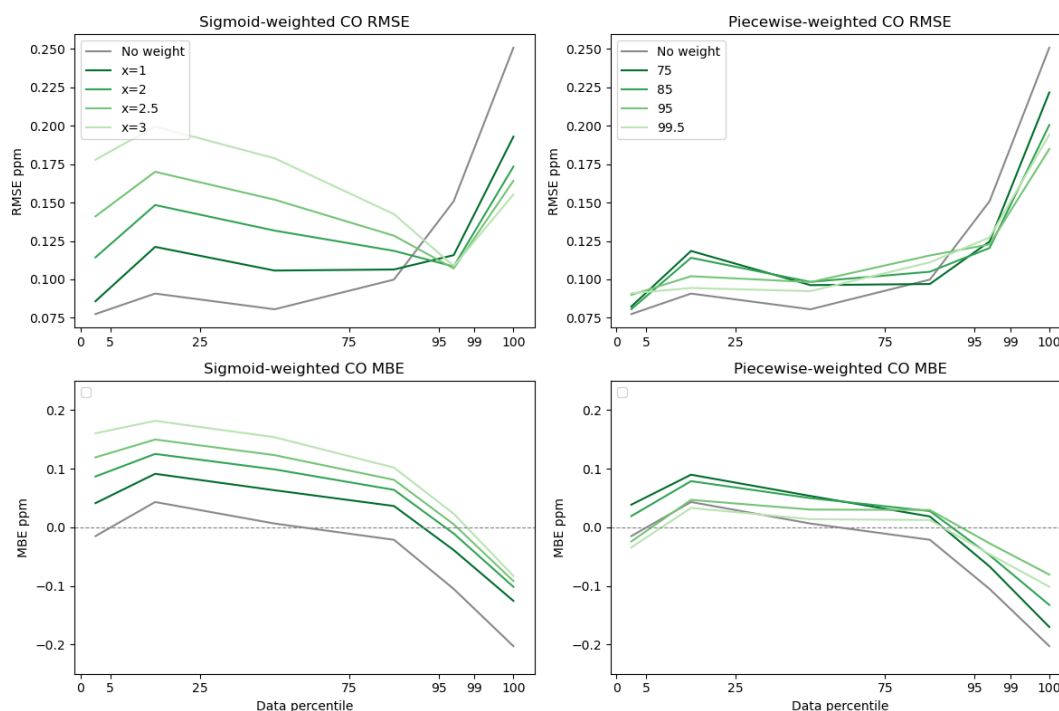


**Figure 4.** CO sensitivity to weighting parameters for MLR models. RMSE and MBE are displayed as a function of data percentile for unweighted data as well as for piecewise and sigmoidal weights. Concentrations of CO range between 0.04 and 1.84 ppm. Lighter colors indicate increased offsets/percentile set points for weighting distributions.

input parameters to model weighting functions is essential in determining the optimal weights and weighting scheme for a colocation data set. When compared to unweighted models, optimal weighting schemes were able to better quantify high concentrations of CO. We further analyzed the  $X_{\text{sigmoid}} = 2$  and  $P_{\text{piecewise}} = 95$ th MLR models as these functions displayed less enhancements in error at baseline values, while they were better when predicting high-concentration data.

As data weighting schemes are implemented (Fig. 5), our model is able to more accurately quantify peaks in both testing and training data. Sigmoidal weighting systematically biases CO measurements, elevating the baseline above actual concentrations (Fig. 5). Piecewise weights improved the prediction of high-concentration CO episodes without systematically skewing lower-concentration measurements (Fig. 5). These techniques allow for improved quantification of high-concentration emission events from urban sources of CO, such as motor vehicle usage and industrial facilities.

### 3.2 CH<sub>4</sub> sensitivity analysis and colocation application

Weighting sensitivity analysis for CH<sub>4</sub> indicated that RF models are better suited for data weighting with the CH<sub>4</sub> data as baseline data in the MLR models showed significantly increased RMSE and MBE with weighting (Figs. 6 and S3–S4). RF models showed less impact on data fits at the baseline, while they still showed decreasing RMSE and MBE

in data above the 95th percentile (Fig. 6). Sigmoid weighting generally performed better for data above the 95th percentile but caused worse fits at the baseline than piecewise weighting (Fig. 6). Reductions in RMSE and MBE generally increased as the offset (sigmoidal weighting) and percentile set point (piecewise weighting) values increased until the 95th percentile. Therefore, we chose to further analyze the  $X_{\text{sigmoid}} = 3$  and  $P_{\text{piecewise}} = 95$ th RF models.

RMSE reductions in data above the 95th percentile ranged from 16%–28% for the chosen weighting models. Sigmoidal  $X_{\text{sigmoid}} = 3$  weighting reduced the MBE of data in the 95th–99th percentile by 72% compared to 47% using piecewise weighting. In both models, reductions in MBE were not as large for data above the 99th percentile (32% for sigmoidal and 20% for piecewise) compared to data in the 95th–99th percentile. Figure 7 illustrates how weighted models underpredict the highest concentrations of CH<sub>4</sub> (above approximately 5 ppm) even as the models better predict elevated concentrations below the highest percentile.

### 3.3 TVOC sensitivity analysis and colocation application

In the TVOC weighting sensitivity test, piecewise-weighting models were less sensitive to weighting changes across MLR and RF models compared to sigmoid-weighting models (Figs. 8 and S5–S6). However, both improved

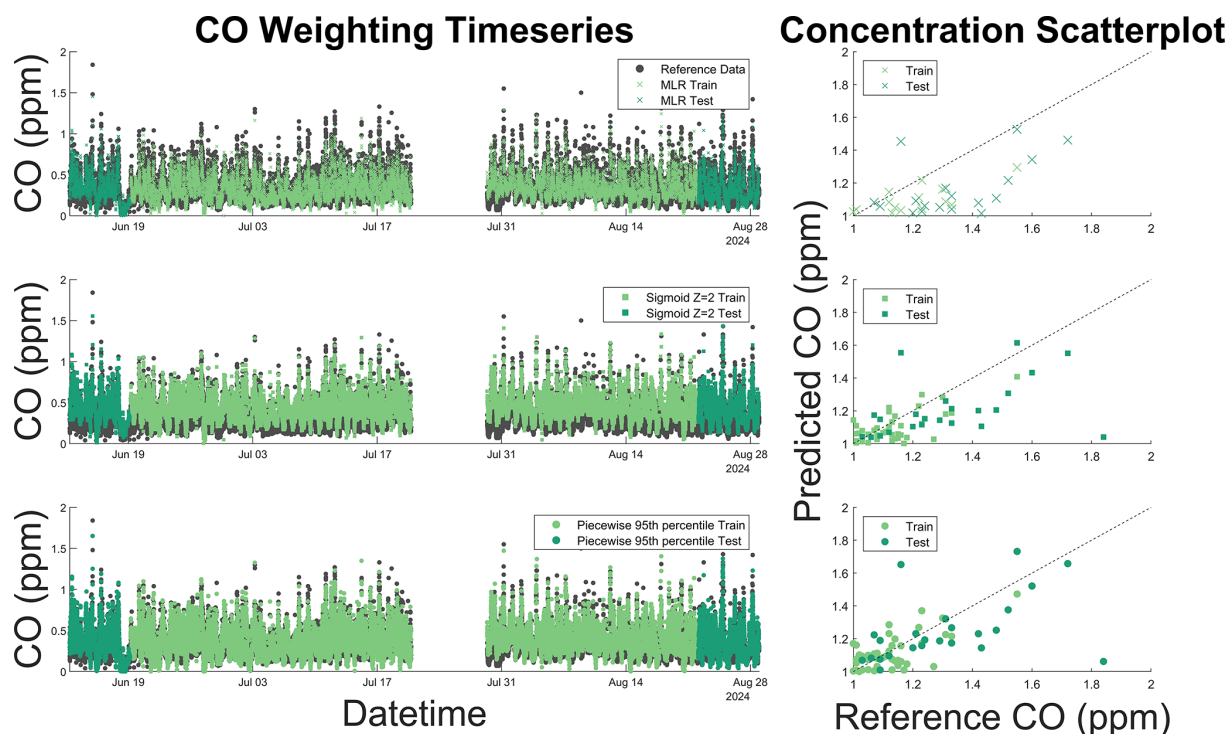


**Figure 5.** CO time series and 1 : 1 scatter plot for unweighted (x) and optimal sigmoidal (square) and piecewise (circle) functions superimposed on reference data (gray). The 1 : 1 line is displayed as a dashed black line on the scatter plot. Dark colors represent testing data and light colors represent training data. Data weights improve our ability to quantify high-concentration pollutant events, with high-concentration peaks displaying improved fits throughout the colocation. However, as is shown in the colocation time series, sigmoid weighting functions shift the baseline, resulting in increased bias and error at low concentrations.

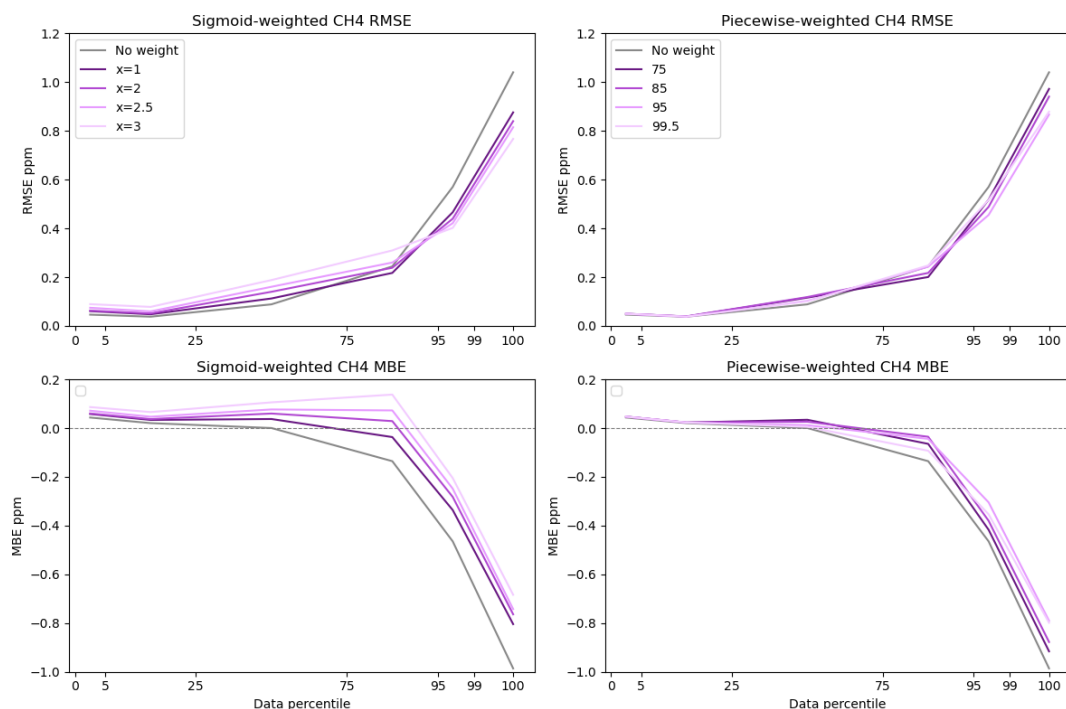


**Figure 6.** CH<sub>4</sub> sensitivity to weighting parameters for RF models. RMSE and MBE are displayed as a function of data percentile for unweighted data as well as for piecewise and sigmoidal weights. Concentrations of CH<sub>4</sub> range between 1.96 and 8.75 ppm. Lighter colors indicate increased offsets/percentile set points for weighting distributions.

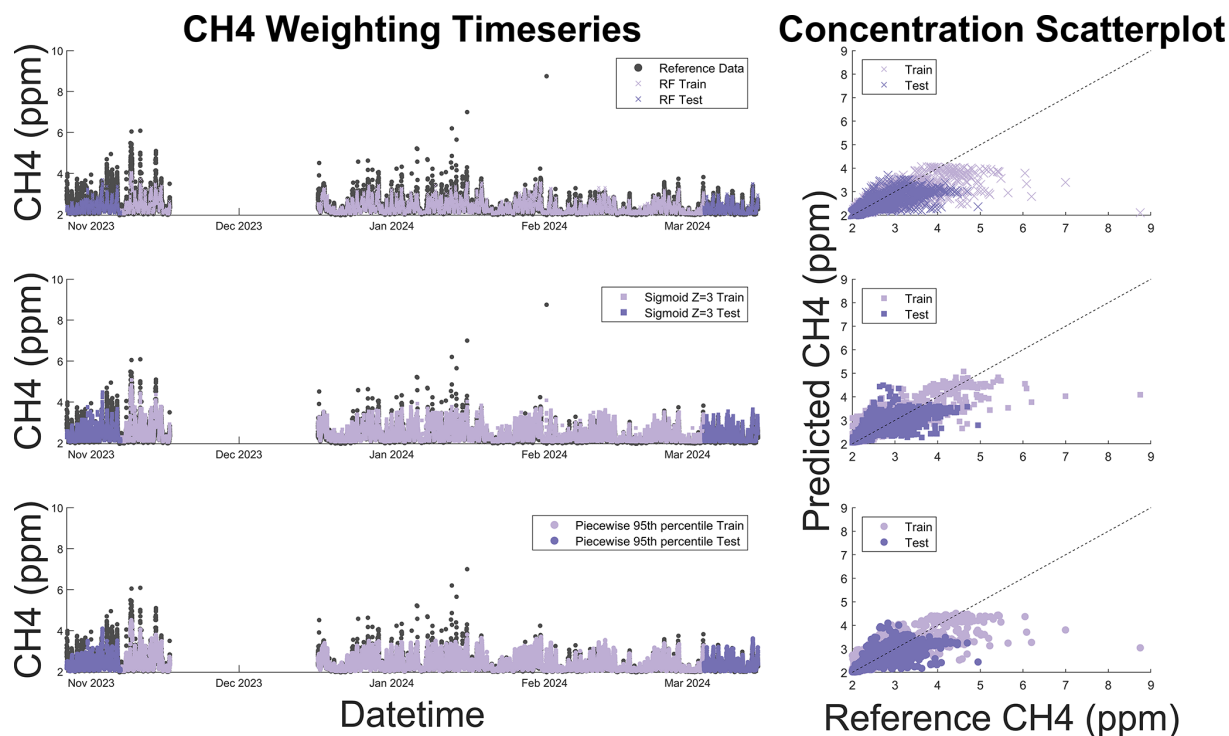


**Figure 7.** CH<sub>4</sub> time series and 1 : 1 scatter plot for unweighted (x) and optimal sigmoidal (square) and piecewise (circle) functions superimposed on reference data (gray). The 1 : 1 line is displayed as a dashed black line on the scatter plot. Dark colors represent testing data and light colors represent training data. The time series plot illustrates that sigmoid and piecewise weights improve our ability to predict high-concentration pollutant events as predicted CH<sub>4</sub> (pink and purple squares and circles) are significantly closer to reference (gray) concentrations when compared to unweighted predictions (pink and purple x's).

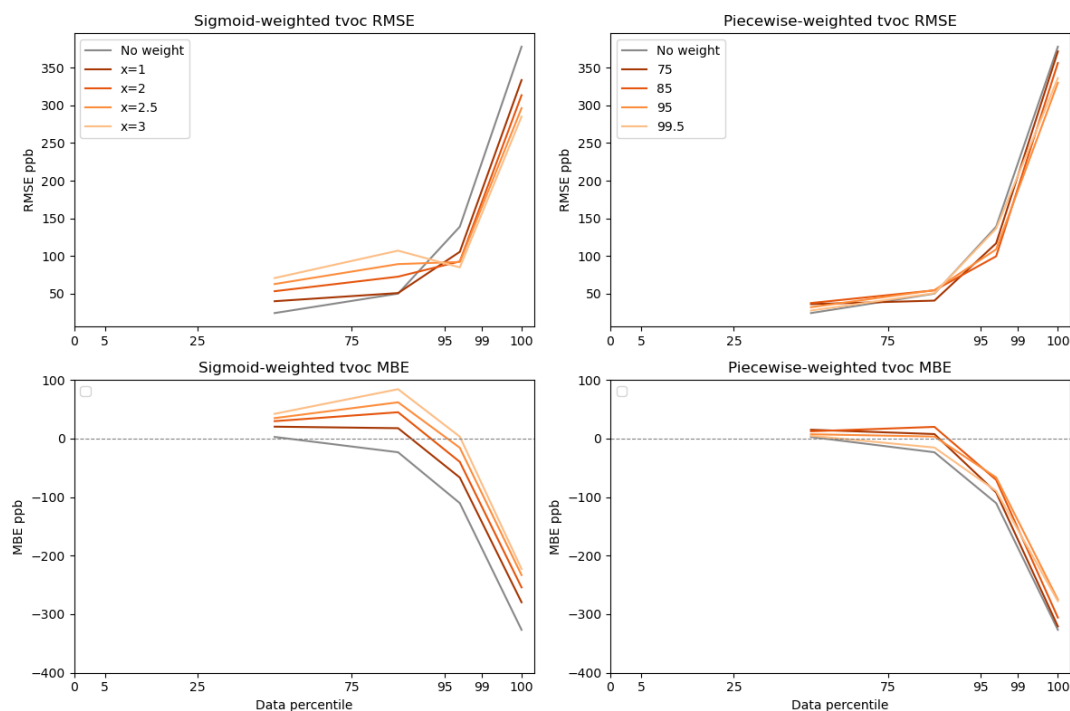


**Figure 8.** TVOC sensitivity to weighting parameters for RF models. RMSE and MBE are displayed as a function of data percentile for unweighted data as well as for piecewise and sigmoidal weights. TVOC concentrations ranged from below the detection limit of the reference instrument (15 ppb) to 2 980 ppb. Lighter colors indicate increased offsets/percentile set points for weighting distributions.



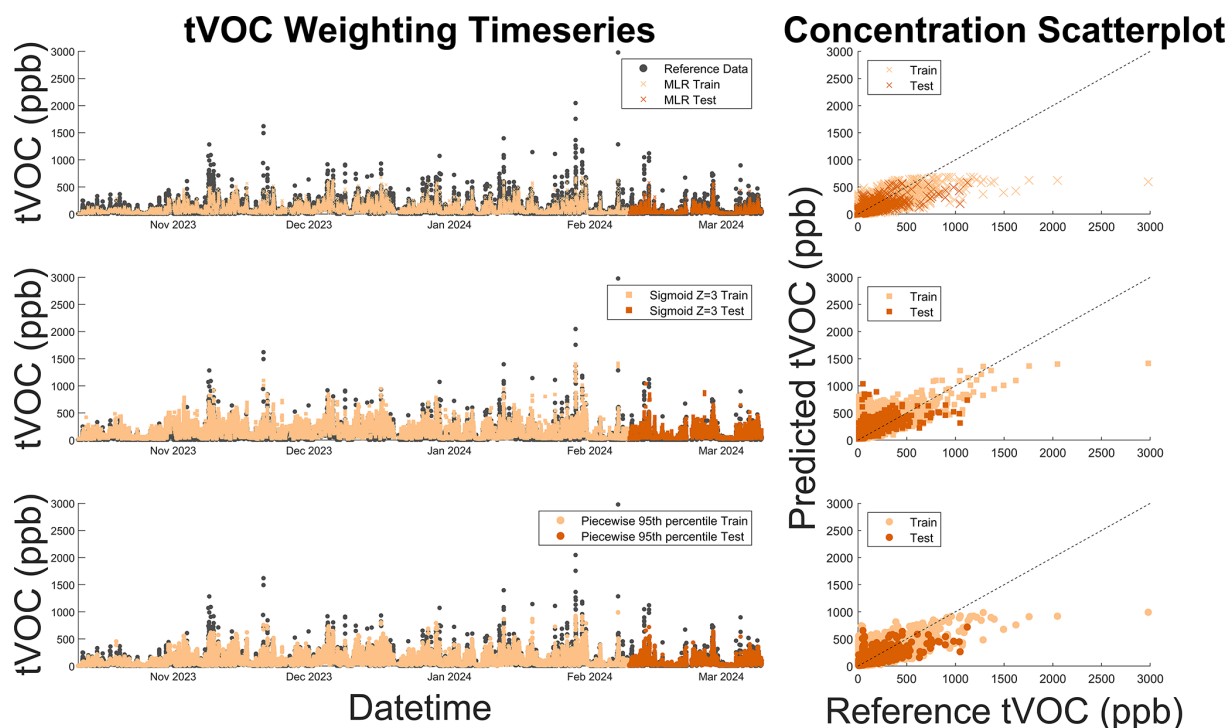


**Figure 9.** TVOC time series and 1 : 1 scatter plot for unweighted (x) and optimal sigmoidal (square) and piecewise (circle) functions superimposed on reference data (gray). The 1 : 1 line is displayed as a dashed black line on the scatter plot. Dark colors represent testing data, and light colors represent training data. As is shown in the time series, the introduction of data weights (light and dark orange circles and squares) allows us to better predict peak reference TVOC concentrations (gray), mitigating the underprediction of high-concentration pollutant spikes when compared to unweighted regression models (light and dark orange x's).

peak concentration predictions compared to the unweighted model (Fig. 9). In subsequent analysis, we focus on the  $P_{\text{piecewise}} = 95\text{th}$  RF model because it best reduced MBE above the 95th percentile of data (Fig. 8). We chose to further investigate the sigmoidal  $X_{\text{sigmoid}} = 3$  RF model because it reduces MBE nearly to zero in the 95th–99th percentiles (Fig. 8). However, sigmoidal  $X_{\text{sigmoid}} = 3$  also caused elevated bias at lower concentrations. In applications where lower-concentration fits are relevant, the sigmoidal  $X_{\text{sigmoid}} = 1$  may be a better choice.

Approximately 29 % of the TVOC reference data is at or below the method detection limit, so RMSE and MBE in the 0th–5th and 5th–25th percentiles are not shown in the figures. Compared to  $\text{CH}_4$  and CO, the TVOC data showed the greatest difference in high-concentration fits between sigmoidal and piecewise weighting. For example, the MBE for data in the 95th–99th percentile and 99th–100th percentile was reduced by 97 % and 32 %, respectively, using sigmoidal weighting compared to just 40 % and 16 % using piecewise weighting. Sigmoidal weighting simultaneously penalizes baseline data while prioritizing high-concentration data, whereas piecewise weighting only weights high-concentration data while treating baseline and interquartile data the same. In a dataset where 29 % of the data is below the detection limit, it appears there is an added

benefit to downweighting the baseline data using sigmoidal weighting.

### 3.4 Discussion general trends

Leveraging data weighting in colocation datasets, we found reductions in both bias and error across peak CO,  $\text{CH}_4$ , and TVOC concentration measurements, especially in the 95–99th percentile of the reference concentrations (Fig. 10). While the 99th–100th percentile data still showed reduced bias and error across all three datasets, the reductions were less significant in the TVOC and  $\text{CH}_4$  data, as indicated by the magnitude of the arrows in Fig. 10. This diminished improvement in 99th+ percentile error and bias may be due to the enhanced variation between data in the top percentile of  $\text{CH}_4$  and TVOC datasets, which, respectively, varied from 3.7–17.6 and 3.6–30.9 standard deviations above the mean (Fig. 2). The top percentile of CO data varied between 3.3 and 8.3 standard deviations above the mean, which accounts for significantly less high-concentration variability than for the other datasets (Fig. 2). Increased variability in pollutant concentrations within the top percentile may result in a poorer fits as even with data weighting, regression models may struggle to fit extreme outliers.

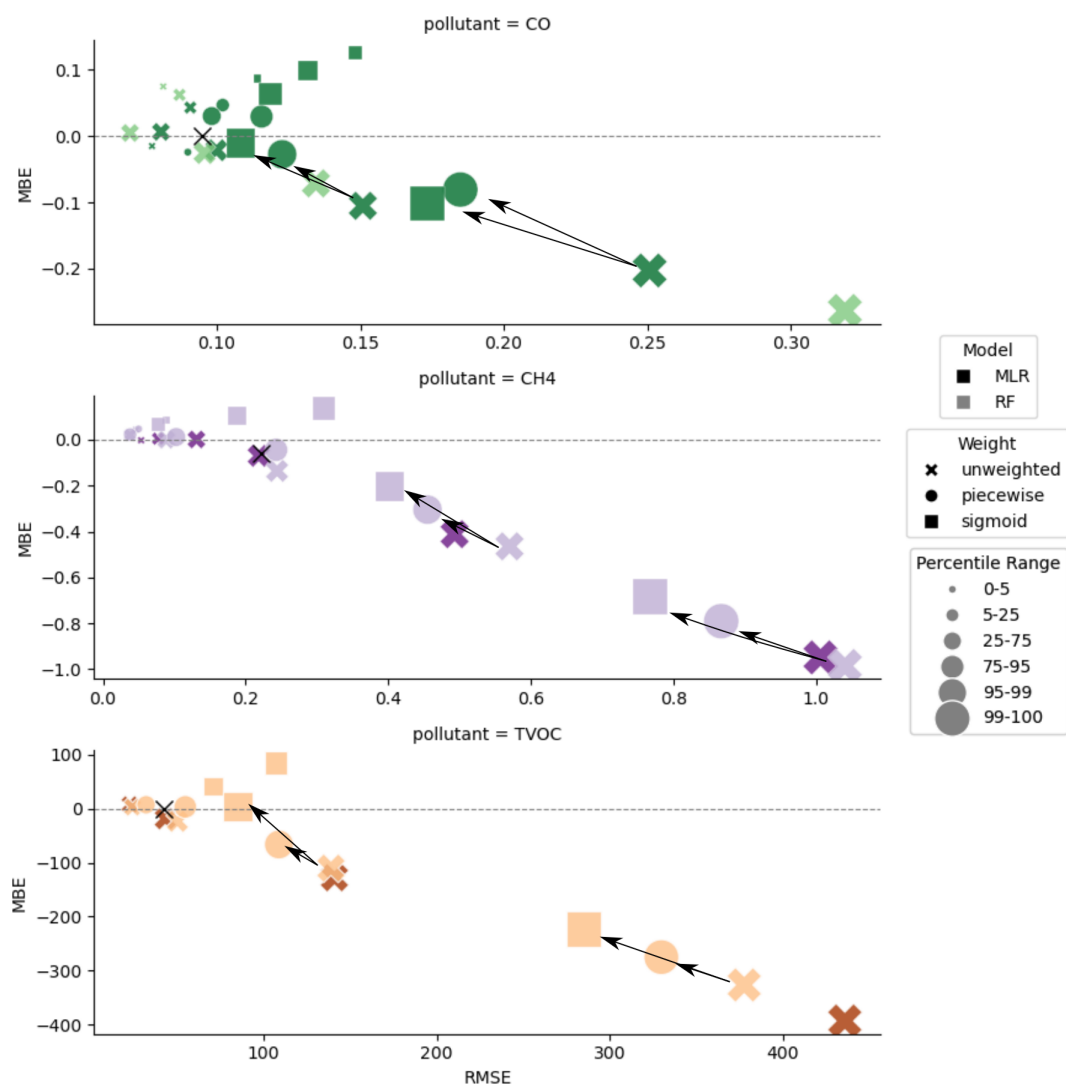


**Figure 10.** CO, CH<sub>4</sub> and TVOC target plot displaying the RMSE and MBE for different data percentiles (marker size). Lighter colors represent RF models and darker colors represent MLR models. Optimal unweighted (x), piecewise (circle), and sigmoidal (square) weighting functions are displayed for each pollutant. The black x indicates the MBE and RMSE of the overall unweighted model, and arrows indicate the direction of improvement at the 95–99th percentiles and 99th+ for the weighted compared to unweighted optimal models.

Though we observed an improvement in our fitting of high-concentration samples, select data points still displayed large discrepancies between reference and predicted concentrations, especially in the highest percentile of data. These results highlight that data weighting methodologies may not ameliorate all causes of concentration underprediction, such as large systematic error as a result of sensor degradation or the LCS not observing the plume. In these cases, further improvements in sensor development and colocation techniques are required. We also note that the large error and bias at the highest percentile of data are not evident in the overall RMSE and MBE values across all three models (indicated with a black “x” in Fig. 10). This is likely because the RMSE and MBE in lower-concentration data mask the high bias and er-

ror in the relatively sparse elevated concentrations. Data partitioning during error analysis proved essential here for fully understanding the performance of the colocation models.

While the sigmoidal weighting scheme was more effective at improving colocation fits for data above the 95th percentile, it also introduced more bias and error at the lower percentiles than the piecewise weighting scheme (Fig. 10). The sigmoidal function assigns a continuous distribution of weights that both penalizes baseline data and prioritizes high-concentration data (Fig. 3). Conversely, the piecewise function prioritizes high-concentration data while treating baseline and interquartile data the same. The trade-off observed in the sigmoidally weighted data may be worthwhile in certain applications where accurate prediction of elevated concen-

trations is pertinent, but error at the baseline is acceptable, such as in pollution event detection and plume prediction (Clements et al., 2024; Kanabkaew et al., 2019; Frischmon et al., 2025a).

The optimal regression model and weighting parameters were unique for each colocation dataset. Even as the datasets showed similar patterns in the sensitivity analysis, each individual pollutant dataset displayed differential sensitivities to changes in input weighting parameters. For example, the unweighted random forest model showed a better fit than unweighted multiple linear regression for CO. However, when applying data weights, the weighted random forest model overfit the CO data, leading to greater reductions in bias and error for the weighted multiple linear regression models. In the TVOC and CH<sub>4</sub> datasets, random forest performed better in both the weighted and unweighted models. These results underscore the importance of testing different weighting schemes on a colocation dataset, as a single one-size-fits-all approach may unnecessarily elevate error at low concentrations and marginally improve fitting at higher pollutant values.

## 4 Conclusions

Employing model weights in ambient gas-phase colocation datasets, we found that data weighting improved our ability to quantify elevated air pollutant concentrations. We assessed the performance of unweighted, sigmoidally weighted, and piecewise weighting schemes in MLR and RF models for CO, TVOC, and CH<sub>4</sub> calibration. MBE was reduced by 16 %–97 %, and RMSE was reduced by 13 %–39 % in concentration data above the 95th percentile when model weights were applied. Our error analysis also underscored the importance of examining statistical metrics for colocation models within partitioned percentile groups as the high error and bias of peak concentration (> 95th percentile) predictions were not evident in the error and bias statistics of the overall models.

Model predictions for weighted CO, TVOC, and CH<sub>4</sub> colocation models were sensitive to changes in our weighting functions, indicating a systematic assessment of optimal weighting parameters is required in each colocation dataset to best identify those that improve high-concentration fitting performance. The optimal regression model and weighting parameters varied between colocation datasets, which reflected the variability in pollutant distributions and sources. Generally, sigmoidal weighting improved high-concentration predictions more than piecewise weighting, but sigmoidal also introduced larger errors and bias for baseline data. The optimal model weight scheme depends on the data application as for some applications, such as emission event detection, accurate prediction of elevated concentrations should be prioritized over baseline concentrations. In the future, we plan to explore how baseline concentra-

tion accuracy might be preserved in a weighted model using a hybrid approach that combines the strengths of both unweighted and sigmoidal weighting schemes.

*Data availability.* The reference CO data were provided courtesy of the Colorado Department of Public Health and Environment, while the reference TVOC and CH<sub>4</sub> data were provided courtesy of the South Coast Air Quality Management District. These data have not passed through the normal review process and are therefore not quality-assured, and they are thus unofficial data. The HAQ-Pod data are available at <https://doi.org/10.17632/fpnh4rztz8.1> (Frischmon et al., 2025b).

*Supplement.* The supplement related to this article is available online at <https://doi.org/10.5194/amt-18-3147-2025-supplement>.

*Author contributions.* Conceptualization: CF and JS; methodology: AG, CF, EM, JP, JS; software: AG, CF, JS; formal analysis: AG, CF, JS; investigation: M.H.; resources: EM, JP, MH; writing and editing: AG, CF, JS; visualization: AG, CF, JS; supervision: MH; project administration: MH; funding acquisition: MH.

*Competing interests.* The contact author has declared that none of the authors has any competing interests.

*Disclaimer.* Publisher's note: Copernicus Publications remains neutral with regard to jurisdictional claims made in the text, published maps, institutional affiliations, or any other geographical representation in this paper. While Copernicus Publications makes every effort to include appropriate place names, the final responsibility lies with the authors.

*Acknowledgements.* Thank you to the Colorado Department of Public Health and Environment and the South Coast Air Quality Monitoring District for reference instrument data, as well as the Utah Department of Environmental Quality for testing initial colocation setups. Thank you to the Hannigan Lab Dev Team (Percy Smith, Spencer Hoehl, Sascha Fowler, and Peter Reeves) for help with troubleshooting and assembling air quality monitors.

*Financial support.* This research has been supported in part by the National Institute of Environmental Health Sciences (NIEHS) (grant no. 1R01ES033478) and by the ASPIRE National Science Foundation (NSF) ERC (grant no. 1941524).

*Review statement.* This paper was edited by Albert Presto and reviewed by two anonymous referees.

## References

- Barkjohn, K. K., Gantt, B., and Clements, A. L.: Development and application of a United States-wide correction for PM<sub>2.5</sub> data collected with the PurpleAir sensor, *Atmos. Meas. Tech.*, 14, 4617–4637, <https://doi.org/10.5194/amt-14-4617-2021>, 2021.
- Bi, J., Wildani, A., Chang, H. H., and Liu, Y.: Incorporating low-cost sensor measurements into high-resolution PM<sub>2.5</sub> modeling at a large spatial scale, *Environ. Sci. Technol.*, 54, 2152–2162, 2020.
- Bigi, A., Mueller, M., Grange, S. K., Ghermandi, G., and Hueglin, C.: Performance of NO, NO<sub>2</sub> low cost sensors and three calibration approaches within a real world application, *Atmos. Meas. Tech.*, 11, 3717–3735, <https://doi.org/10.5194/amt-11-3717-2018>, 2018.
- Casey, J. G. and Hannigan, M. P.: Testing the performance of field calibration techniques for low-cost gas sensors in new deployment locations: across a county line and across Colorado, *Atmos. Meas. Tech.*, 11, 6351–6378, <https://doi.org/10.5194/amt-11-6351-2018>, 2018.
- Casey, J. G., Collier-Oxandale, A., and Hannigan, M.: Performance of artificial neural networks and linear models to quantify 4 trace gas species in an oil and gas production region with low-cost sensors, *Sensor. Actuat. B-Chem.*, 283, 504–514, 2019.
- Clements, D., Coburn, M., Cox, S. J., Bulot, F. M. J., Xie, Z.-T., and Vanderwel, C.: Comparing Large-Eddy Simulation and Gaussian Plume Model to Sensor Measurements of an Urban Smoke Plume, *Atmosphere*, 15, 1089, <https://doi.org/10.3390/atmos15091089>, 2024.
- Collier-Oxandale, A., Casey, J. G., Piedrahita, R., Ortega, J., Halliday, H., Johnston, J., and Hannigan, M. P.: Assessing a low-cost methane sensor quantification system for use in complex rural and urban environments, *Atmos. Meas. Tech.*, 11, 3569–3594, <https://doi.org/10.5194/amt-11-3569-2018>, 2018.
- De Mesnard, L.: Pollution models and inverse distance weighting: Some critical remarks, *Comput. Geosci.*, 52, 459–469, 2013.
- Frischmon, C., Crosslin, J., Burks, L., Weckesser, B., Hannigan, M., and Duderstadt, K.: Detecting air pollution episodes and exploring their impacts using low-cost sensor data and simultaneous community symptom and odor reports, *Environ. Res. Lett.*, 20, 044043, <https://doi.org/10.1088/1748-9326/adc28a>, 2025a.
- Frischmon, C., Silberstein, J., and Hannigan, M.: Low-cost sensor data for data weighting, V1, Mendeley Data [data set], <https://doi.org/10.17632/fpnh4rztz8.1>, 2025b.
- Furuta, D., Sayahi, T., Li, J., Wilson, B., Presto, A. A., and Li, J.: Characterization of inexpensive metal oxide sensor performance for trace methane detection, *Atmos. Meas. Tech.*, 15, 5117–5128, <https://doi.org/10.5194/amt-15-5117-2022>, 2022.
- Gonzalez, A., Boies, A., Swason, J., and Kittelson, D.: Field Calibration of Low-Cost Air Pollution Sensors, *Atmos. Meas. Tech. Discuss.* [preprint], <https://doi.org/10.5194/amt-2019-299>, 2019.
- Hallios, C. H., Landeg-Cox, C., Lowther, S. D., Middleton, A., Marczylo, T., and Dimitroulopoulou, S.: Chemicals in European residences – Part I: A review of emissions, concentrations and health effects of volatile organic compounds (VOCs), *Sci. Total Environ.*, 839, 156201, <https://doi.org/10.1016/j.scitotenv.2022.156201>, 2022.
- Jayarathne, R., Liu, X., Thai, P., Dunbabin, M., and Morawska, L.: The influence of humidity on the performance of a low-cost air particle mass sensor and the effect of atmospheric fog, *Atmos. Meas. Tech.*, 11, 4883–4890, <https://doi.org/10.5194/amt-11-4883-2018>, 2018.
- Kanabkaew, T., Mekbungwan, P., Raksakietisak, S., and Kanchanasut, K.: Detection of PM<sub>2.5</sub> plume movement from IoT ground level monitoring data, *Environ. Pollut.*, 252, 543–552, <https://doi.org/10.1016/j.envpol.2019.05.082>, 2019.
- Karagulian, F., Barbieri, M., Kotsev, A., Spinelle, L., Gerboles, M., Lagler, F., Redon, N., Crunaire, S., and Borowiak, A.: Review of the performance of low-cost sensors for air quality monitoring, *Atmosphere*, 10, 506, <https://doi.org/10.3390/atmos10090506>, 2019.
- Levy Zamora, M., Buehler, C., Datta, A., Gentner, D. R., and Koehler, K.: Identifying optimal co-location calibration periods for low-cost sensors, *Atmos. Meas. Tech.*, 16, 169–179, <https://doi.org/10.5194/amt-16-169-2023>, 2023.
- Liang, L.: Calibrating low-cost sensors for ambient air monitoring: Techniques, trends, and challenges, *Environ. Res.*, 197, 111163, <https://doi.org/10.1016/j.envres.2021.111163>, 2021.
- Liu, D., Di, B., Luo, Y., Deng, X., Zhang, H., Yang, F., Grieneisen, M. L., and Zhan, Y.: Estimating ground-level CO concentrations across China based on the national monitoring network and MOPITT: potentially overlooked CO hotspots in the Tibetan Plateau, *Atmos. Chem. Phys.*, 19, 12413–12430, <https://doi.org/10.5194/acp-19-12413-2019>, 2019.
- Liu, N., Bu, Z., Liu, W., Kan, H., Zhao, Z., Deng, F., Huang, C., Zhao, B., Zeng, X., Sun, Y., Qian, H., Mo, J., Sun, C., Guo, J., Zheng, X., Weschler, L. B., and Zhang, Y.: Health effects of exposure to indoor volatile organic compounds from 1980 to 2017: a systematic review and meta-analysis, *Indoor Air*, 32, e13038, <https://doi.org/10.1111/ina.13038>, 2022.
- Magi, B. I., Cupini, C., Francis, J., Green, M., and Hauser, C.: Evaluation of PM<sub>2.5</sub> measured in an urban setting using a low-cost optical particle counter and a Federal Equivalent Method Beta Attenuation Monitor, *Aerosol Sci. Tech.*, 54, 147–159, 2020.
- Malings, C., Tanzer, R., Haurlyliuk, A., Saha, P. K., Robinson, A. L., Presto, A. A., and Subramanian, R.: Fine particle mass monitoring with low-cost sensors: Corrections and long-term performance evaluation, *Aerosol Sci. Tech.*, 54, 160–174, 2020.
- Mead, M., Popoola, O., Stewart, G., Landshoff, P., Calleja, M., Hayes, M., Baldovi, J., McLeod, M., Hodgson, T., Dicks, J., Lewis, A., Cohen, J., Baron, R., Saffell, J. R., and Jones, R. L.: The use of electrochemical sensors for monitoring urban air quality in low-cost, high-density networks, *Atmos. Environ.*, 70, 186–203, 2013.
- Mei, H., Han, P., Wang, Y., Zeng, N., Liu, D., Cai, Q., Deng, Z., Wang, Y., Pan, Y., and Tang, X.: Field evaluation of low-cost particulate matter sensors in Beijing, *Sensors*, 20, 4381, <https://doi.org/10.3390/s20164381>, 2020.
- Morawska, L., Thai, P. K., Liu, X., Asumadu-Sakyi, A., Ayoko, G., Bartonova, A., Bedini, A., Chai, F., Christensen, B., Dunbabin, M., Gao, J., Hagler, G. S., Jayaratne, R., Kumar, P., Lau, A. K., Louie, P. K., Mazaheri, M., Ning, Z., Motta, N., Mullins, B., Rahman, M. M., Ristovski, Z., Shafei, M., Tjondronegoro, D., Westerdahl, D., and Williams, R.: Applications of low-cost sensing technologies for air quality monitoring and exposure assessment: How far have they gone?, *Environ. Int.*, 116, 286–299, <https://doi.org/10.1016/j.envint.2018.04.018>, 2018.
- Okorn, K. and Hannigan, M.: Applications and Limitations of Quantifying Speciated and Source-Appportioned

- VOCs with Metal Oxide Sensors, *Atmosphere*, 12, 1383, <https://doi.org/10.3390/atmos12111383>, 2021a.
- Okorn, K. and Hannigan, M.: Improving Air Pollutant Metal Oxide Sensor Quantification Practices through: An Exploration of Sensor Signal Normalization, Multi-Sensor and Universal Calibration Model Generation, and Physical Factors Such as Co-Location Duration and Sensor Age, *Atmosphere*, 12, 645, <https://doi.org/10.3390/atmos12050645>, 2021b.
- Rai, A. C., Kumar, P., Pilla, F., Skouloudis, A. N., Di Sabatino, S., Ratti, C., Yasar, A., and Rickerby, D.: End-user perspective of low-cost sensors for outdoor air pollution monitoring, *Sci. Total Environ.*, 607, 691–705, 2017.
- Raub, J.: Health effects of exposure to ambient carbon monoxide, *Chemosphere - Global Change Science*, 1, 331–351, 1999.
- Rose, N., Cowie, C., Gillett, R., and Marks, G. B.: Weighted road density: A simple way of assigning traffic-related air pollution exposure, *Atmos. Environ.*, 43, 5009–5014, 2009.
- Sadighi, K., Coffey, E., Polidori, A., Feenstra, B., Lv, Q., Henze, D. K., and Hannigan, M.: Intra-urban spatial variability of surface ozone in Riverside, CA: viability and validation of low-cost sensors, *Atmos. Meas. Tech.*, 11, 1777–1792, <https://doi.org/10.5194/amt-11-1777-2018>, 2018.
- Sayahi, T., Butterfield, A., and Kelly, K.: Long-term field evaluation of the Plantower PMS low-cost particulate matter sensors, *Environ. Pollut.*, 245, 932–940, 2019.
- Silberstein, J., Wellbrook, M., and Hannigan, M.: Utilization of a Low-Cost Sensor Array for Mobile Methane Monitoring, *Sensors*, 24, 519, <https://doi.org/10.3390/s24020519>, 2024.
- Susan, S. and Kumar, A.: The balancing trick: Optimized sampling of imbalanced datasets—A brief survey of the recent State of the Art, *Engineering Reports*, 3, e12298, <https://doi.org/10.1002/eng2.12298>, 2021.
- Tancev, G.: Relevance of drift components and unit-to-unit variability in the predictive maintenance of low-cost electrochemical sensor systems in air quality monitoring, *Sensors*, 21, 3298, <https://doi.org/10.3390/s21093298>, 2021.
- Tang, D., Zhan, Y., and Yang, F.: A review of machine learning for modeling air quality: Overlooked but important issues, *Atmos. Res.*, 300, 107261, <https://doi.org/10.1016/j.atmosres.2024.107261>, 2024.
- Thorson, J., Collier-Oxandale, A., and Hannigan, M.: Using a low-cost sensor array and machine learning techniques to detect complex pollutant mixtures and identify likely sources, *Sensors*, 19, 3723, <https://doi.org/10.3390/s19173723>, 2019.
- Wei, P., Ning, Z., Ye, S., Sun, L., Yang, F., Wong, K. C., Westerdahl, D., and Louie, P. K.: Impact analysis of temperature and humidity conditions on electrochemical sensor response in ambient air quality monitoring, *Sensors*, 18, 59, <https://doi.org/10.3390/s18020059>, 2018.
- Xing, Y.-F., Xu, Y.-H., Shi, M.-H., and Lian, Y.-X.: The impact of PM<sub>2.5</sub> on the human respiratory system, *J. Thorac. Dis.*, 8, E69–E74, <https://doi.org/10.3978/j.issn.2072-1439.2016.01.19>, 2016.
- Zhang, H., Hu, J., Qi, Y., Li, C., Chen, J., Wang, X., He, J., Wang, S., Hao, J., Zhang, L., Zhang, L., Zhang, Y., Li, R., Wang, S., and Chai, F.: Emission characterization, environmental impact, and control measure of PM<sub>2.5</sub> emitted from agricultural crop residue burning in China, *J. Clean. Prod.*, 149, 629–635, 2017.
- Zhou, X., Zhou, X., Wang, C., and Zhou, H.: Environmental and human health impacts of volatile organic compounds: A perspective review, *Chemosphere*, 313, 137489, <https://doi.org/10.1016/j.chemosphere.2022.137489>, 2023.
- Zimmerman, N., Presto, A. A., Kumar, S. P. N., Gu, J., Hauryliuk, A., Robinson, E. S., Robinson, A. L., and R. Subramanian: A machine learning calibration model using random forests to improve sensor performance for lower-cost air quality monitoring, *Atmos. Meas. Tech.*, 11, 291–313, <https://doi.org/10.5194/amt-11-291-2018>, 2018.